

$$\varphi_\alpha(\rho, \theta) = a_1 \varphi_1(\rho, \theta) + a_2 \varphi_2(\rho, \theta), \quad r^{1/2} \leq \rho \leq 1,$$

$$\varphi_\beta(\rho, \theta) = b_1 \varphi_1\left(\frac{r}{\rho}, \theta\right) + b_2 \varphi_2\left(\frac{r}{\rho}, \theta\right), \quad r \leq \rho \leq r^{1/2}, \quad (4.3)$$

where the coefficients a_1, a_2, b_1, b_2 are

$$a_1 = \frac{2\mu_\beta}{\mu_\alpha + \mu_\beta}, \quad a_2 = \frac{\mu_\alpha - \mu_\beta}{\mu_\alpha + \mu_\beta},$$

$$b_1 = -\frac{2\mu_\alpha}{\mu_\alpha + \mu_\beta}, \quad b_2 = \frac{\mu_\alpha - \mu_\beta}{\mu_\alpha + \mu_\beta}. \quad (4.4)$$

The field solutions (4.3), (4.4) can be verified, with some mathematical skills, that they indeed fulfill Laplace equation, the traction-free boundary condition (2.1) as well as the continuity conditions of the warping displacement and traction at interface $\rho = r^{1/2}$, namely

$$w_\alpha - \left(\frac{\mu_\alpha + \mu_\beta}{2\mu_\alpha} w_\beta + \frac{\mu_\alpha - \mu_\beta}{2\mu_\alpha} \bar{w}_\beta \right) = i \frac{\mu_\alpha - \mu_\beta}{2\mu_\alpha} z \bar{z}. \quad (4.5)$$

We now consider a special type of two-phase elliptical hollow section. Suppose the geometry of this compound elliptical section is given such a way that, under the transformation (3.1), it is mapped onto the configuration of the auxiliary boundary value problem. We claim that the warping functions of this compound elliptical cross-section in the p -plane are given as (4.3) and (4.4). The reasons are simple. Since φ is the real part of the analytic function w and the mapping function (3.1), and its inverse, is analytic, thus it satisfies the governing equation (Laplace equations). Also, since for a hollow confocal ellipse, the closed contour $\rho = r^{1/2}$ has zero warping (or equivalently the normal derivative of the conjugate function ψ is zero). Thus, Packham and Shail's superposition method is applicable to this compound confocally elliptical configurations. Obviously (4.3) and (4.4) are exactly the warping fields of this compound elliptical section in the transformed domain. This perspective is new and may have further implications on chessboard-like elliptical geometry [17]. Of course, the torsion solutions of this compound elliptical section could have been analyzed directly as in the steps in Section 2 together with the satisfaction of interface conditions (4.5). Although much cumbersome than that of (4.3)–(4.4), we have indeed done the analysis and have verified that the superposition is true for this configuration.

Acknowledgments

This work was supported by the National Science Council, Taiwan, under contract NSC 90-2211-E006-119.

References

- [1] Sokolnikoff, I. S., 1956, *Mathematical Theory of Elasticity*, McGraw-Hill, New York.
- [2] Chiskis, A., and Parnes, R., 2000, "On Torsion of Closed Thin-Wall Members With Arbitrary Stress-Strain Laws: A General Criterion for Cross Sections Exhibiting No Warping," *ASME J. Appl. Mech.*, **67**, pp. 460–464.
- [3] Packham, B. A., and Shail, R., 1978, "St. Venant Torsion of Composite Cylinders," *J. Elast.*, **8**, pp. 393–407.
- [4] Ahlfors, L. V., 1966, *Complex Analysis: An Introduction to the Theory of Analytic Functions of One Complex Variable*, McGraw-Hill, Tokyo.
- [5] Caratheodory, C., 1969, *Conformal Representation*, Cambridge University Press, Cambridge, UK.
- [6] Chen, T., Benveniste, Y., and Chuang, P. C., 2002, "Exact Solutions in Torsion of Composite Bars: Thickly Coated Neutral Inhomogeneities and Composite Cylinder Assemblages," *Proc. R. Soc. London, Ser. A*, **458**, pp. 1719–1759.
- [7] Wang, C. T., 1953, *Applied Elasticity*, McGraw-Hill, New York.
- [8] Muskhelishvili, N. I., 1953, *Some Basic Problems of the Mathematical Theory of Elasticity*, Noordhoff, Groningen.
- [9] Lurie, A. I., 1970, *Theory of Elasticity*, Nauka, Moscow (in Russian).
- [10] Bartels, R. C. F., 1943, "Torsion of Hollow Cylinders," *Trans. Am. Math. Soc.*, **53**, pp. 1–13.
- [11] Greenhill, A. G., 1879, "Fluid Motion Between Confocal Elliptic Cylinders and Confocal Ellipsoids," *Q. J. Math.*, **16**, pp. 227–256.
- [12] Love, A. E. H., 1944, *A Treatise on the Mathematical Theory of Elasticity*, Dover, New York.

- [13] Timoshenko, S. P., and Goodier, J. N., 1970, *Theory of Elasticity*, 3rd Ed., McGraw-Hill, New York.
- [14] Packham, B. A., and Shail, R., 1971, "Stratified Laminar Flow of Two Immiscible Fluids," *Proc. Cambridge Philos. Soc.*, **69**, pp. 443–448.
- [15] Chen, T., and Huang, Y. L., 1998, "Saint-Venant Torsion of a Two-Phase Circumferentially Symmetric Compound Bar," *J. Elast.*, **53**, pp. 109–124.
- [16] Kellogg, O. D., 1953 *Foundations of Potential Theory*, Dover, New York.
- [17] Chen, T., 2001, "Torsion of a Rectangular Checkerboard and the Analogy Between Rectangular and Curvilinear Cross-Sections," *Q. J. Mech. Appl. Math.*, **54**, pp. 227–241.

Are Lower-Order Gradient Theories of Plasticity Really Lower Order?

K. Yu. Volokh

Faculty of Civil Engineering, Technion–Israel Institute of Technology, Haifa 32000, Israel

J. W. Hutchinson¹

Division of Engineering and Applied Sciences, Harvard University, Cambridge, MA 02138

e-mail: hutchinson@husm.harvard.edu. Mem. ASME

An explicit example of one-dimensional shearing is used to illustrate the necessity of extra boundary conditions for a class of incremental theories of plasticity regarded as otherwise conventional apart from a dependence of the tangential moduli on gradients of plastic strain. [DOI: 10.1115/1.1504096]

Gradient effects may be introduced into plasticity theory by using additional kinematical and work-conjugate stress variables. Such theories enjoy the structure of Cosserat-type continua in the general case. Extra stresses and boundary conditions are inherent in the generalized continuum theories. While very flexible in introducing new quantities, the generalized continuum theories have drawbacks associated with the difficulty of physical interpretation of the higher-order stresses and extra boundary conditions. To avoid such higher-order formulations, a class of theories has been proposed by Bassani [1], which introduces gradients of plastic strain into the instantaneous tangent moduli. Otherwise, conventional equilibrium equations of lower-order theory are retained. The underlying premise of these enhanced conventional theories is that they accommodate only the same types of boundary conditions associated with the conventional theory. In this note it will be shown that this is not always the case. By considering a relatively simple, well-posed problem for one-dimensional shearing of a layer, it will be demonstrated that this class of theories can accommodate extra boundary conditions under special circumstances, and, in fact, are not lower order in this sense. However, the higher-order nature of the theories does not appear to be in accord with basic physical requirements, as will be discussed.

To begin, consider a conventional material whose stress-strain curve in shear is specified by $\gamma \equiv \gamma_e + \gamma_p = \tau/G + \gamma_p$ with

$$\gamma_p = 0 (\tau \leq \tau_Y), \quad \gamma_p = \gamma_0 (\tau/\tau_Y - 1)^n (\tau > \tau_Y). \quad (1)$$

In the plastic range $\tau/\tau_Y = 1 + (\gamma_p/\gamma_0)^N$ with $N = 1/n$, such that the tangent modulus defined by $\dot{\tau} = G_t \dot{\gamma}$ can be expressed as

$$\frac{1}{G_t} = \frac{1}{G} + \frac{1}{H} \quad \text{with} \quad \frac{1}{H} = \frac{n\gamma_0}{\tau_Y} \left(\frac{\gamma_p^2}{\gamma_0^2} \right)^{(n-1)/2n}. \quad (2)$$

¹To whom correspondence should be addressed.

Contributed by the Applied Mechanics Division of THE AMERICAN SOCIETY OF MECHANICAL ENGINEERS for publication in the JOURNAL OF APPLIED MECHANICS. Manuscript received by the ASME Applied Mechanics Division, June 21, 2001; final revision, June 8, 2002. Associate Editor: A. Needleman.

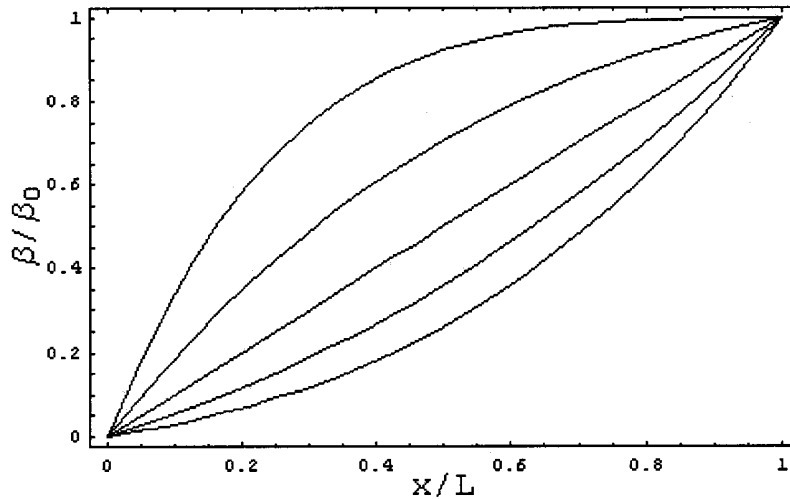


Fig. 1 Numerical solutions of Eq. (4) with $n=3$ and $m=2$. The curves correspond to the values $\lambda=1/4; 1/2; 1; 2; 4$ from the bottom to the top.

Consider shearing displacements parallel to the x_2 -axis with $u_2(x_1) \equiv u(x)$ and $\gamma(x) = u'(x)$. With $\sigma_{12}(x_1) \equiv \tau(x)$, conventional incremental equilibrium requires $\dot{\tau}'(x) = 0$.

The incremental boundary value problem considered here has displacement boundary conditions: $\dot{u}(0) = 0$ and $\dot{u}(L) = \dot{v}$ with v increased monotonically. The solution for the conventional material where the stress satisfies (1) is a uniform state of stress and strain consistent with the incremental relations $\dot{\gamma} = \dot{v}/L$ and $\dot{u} = \dot{\gamma}x$. The plastic strain is also uniform and all details of the solution can be generated as a function of v .

Introduce the enhanced material by including the gradient of plastic strain in the tangent modulus in (2) according to

$$\frac{1}{G_t} = \frac{1}{G} + \frac{1}{H} \quad \text{with} \quad \frac{1}{H} = \frac{n\gamma_0}{\tau_Y} \left(\frac{(\gamma_p/\gamma_0)^2}{(1 + \ell^2 \gamma_p'^2/\gamma_p^2)^m} \right)^{(n-1)/2n} \quad (3)$$

where ℓ is the material length parameter. The factor m can be used to adjust the strength of the gradient hardening. In the absence of the gradient this reduces to the original form (2), and it meets requirements outlined for the type of formulation proposed by Bassani [1]. In the plastic range, $\dot{\tau} = G_t \dot{\gamma}$ is precisely equivalent to $\dot{\tau} = H \dot{\gamma}_p$. Assuming conventional equilibrium holds ($\dot{\tau}'(x) = 0$), $\dot{\tau}$ is uniform and, thus, $\dot{\gamma}_e$ is uniform in both the elastic and plastic range. In the elastic range ($\tau \leq \tau_Y$), $\gamma = \gamma_e = v/L$, $\tau = G\gamma$ and $\gamma_p = 0$. In the plastic range ($\tau > \tau_Y$), equilibrium requires $(H \dot{\gamma}_p)' = 0$. Because $\dot{\gamma}_e$ is uniform, the displacement can be written as $u(v, x) = \gamma_e(v)x + u_p(v, x)$ with $\gamma_p = u_p'$. Moreover, because H is homogeneous in the plastic strain and its gradient, the equation $(H \dot{\gamma}_p)' = 0$ admits a separated solution $u_p = \alpha(v)\beta(x)$ with $\gamma_p = \alpha\beta'$ and $\dot{\gamma}_p = \dot{\alpha}\beta'$ ($\dot{\alpha} = d\alpha/dv$). The equation is third order and homogeneous in β and its derivatives:

$$\beta''[(n-1)m\ell^2\beta'''\beta' + [1 - (n-1)m]\ell^2\beta''^2 + \beta'^2] = 0. \quad (4)$$

One solution to (4) is obviously $\beta' = c$ corresponding to a uniform plastic strain distribution. This solution coincides with the solution for the conventional material when the conditions, $\dot{u}(0) = 0$ and $\dot{u}(L) = \dot{v}$, are enforced. But there is an entire family of other perfectly acceptable solutions to the problem as posed that satisfy the boundary conditions $\dot{u}(0) = 0$ and $\dot{u}(L) = \dot{v}$. These solutions do not have a uniform distribution of plastic strain. They are possible because $\dot{\gamma}_p$ is not otherwise determined at the onset of plastic flow. Due to the third-order character of (4), one additional boundary condition can be imposed. The example shown in Fig. 1 was computed numerically from (4) with $\beta(0) = 0$, $\beta(L)$

$= \beta_0$ and $\beta'(0) = \lambda\beta_0/L$ for $n=3$, $m=2$, $\ell/L=1$ and several values of λ . The solution for $\lambda=1$ is that with uniform plastic strain. For each of the solutions, it is a straightforward process to piece together the entire solution to the boundary value problem with $\dot{u}(0) = 0$ and $\dot{u}(L) = \dot{v}$ by making an appropriate choice for $\alpha(v)$. The plastic strain distribution will depend on λ , as will the overall relation between shear stress and shearing displacement v .

Uniqueness of solution requires that one extra boundary condition be specified on $\dot{\gamma}_p$ in addition to $\dot{u}(0) = 0$ and $\dot{u}(L) = \dot{v}$. The example shown introduces the extra condition at the left end of the interval. One could have equally well imposed the one extra boundary condition at the right end, but not on both simultaneously. Higher order theories (Fleck and Hutchinson [2] and Hutchinson [3]) do involve extra boundary conditions. In a one-dimensional problem such as the present one, they require specification of extra conditions at *both* ends of the interval. An extra condition at each end of the interval would be expected on physical grounds due to the constraint, or lack thereof, on plastic flow that would be expected due to interaction of dislocations with each boundary. Thus, it would appear that the added flexibility associated with the extra boundary condition afforded by the enhanced formulation in the present example is inconsistent with sound physical principles.

The values of parameters chosen for the numerical example in Fig. 1 are not exceptional; solutions can be generated for any choice of the parameters. Similarly, the one-dimensional shearing problem is not an isolated example. Another simple, basic example for which an extra boundary condition must be specified is the deformation well away from the edges of a uniform film attached to a planar substrate. Moreover, the issue arises in this enhanced class of conventional theories whether these problems are approached using a phenomenological theory or a single crystal theory such as that discussed by Bassani [1]. The need for an extra boundary condition in these examples arises because the deformation at the onset of plasticity is uniform and, therefore, the gradient of plastic strain is indeterminate. Consequently the tangent modulus is also indeterminate unless an additional condition is imposed such as the extra boundary condition. At the very least, these basic examples raise questions about enhanced conventional formulations, and they suggest that further conditions must be stated to render unique solutions. Our own view is that higher-order boundary conditions, which specify constraints on plastic deformation at boundaries, interfaces, and free surfaces, should be an integral part of a strain gradient theory of plasticity.

Acknowledgment

The work of KYV was supported by the Fund for the Promotion of Research at the Technion.

References

- [1] Bassani, J. L., 2001, "Incompatibility and Simple Gradient Theory of Plasticity," *J. Mech. Phys. Solids*, **49**, pp. 1983–1996.
- [2] Fleck, N. A., and Hutchinson, J. W., 2001, "A Reformulation of Strain Gradient Plasticity," *J. Mech. Phys. Solids*, **49**, pp. 2245–2271.
- [3] Hutchinson, J. W., 2000, "Plasticity at the Micron Scale," *Int. J. Solids Struct.*, **37**, pp. 225–238.

A Note on the Post-Flutter Dynamics of a Rotating Disk

A. Raman¹

School of Mechanical Engineering, Purdue University,
West Lafayette, IN 47907-1288
e-mail: raman@ecn.purdue.edu

M. H. Hansen

Wind Energy Department Risø National Laboratory, DK-4000 Roskilde, Denmark

C. D. Mote, Jr.

Professor of Engineering and President,
Glenn L. Martin Institute, University of Maryland,
College Park, MD 20742

The dynamic response of a thin, flexible disk spinning in an enclosed air-filled chamber, beyond the onset of aeroelastic flutter, is investigated experimentally. The results describe the occurrence of new nonlinear dynamic phenomena in the post-flutter regime. A primary instability leads to the Hopf bifurcation of the flat equilibrium to a finite amplitude backward traveling wave. A secondary instability causes this traveling wave to jump to a large-amplitude frequency locked, traveling wave vibration. For a small range of rotation speeds, both types of traveling wave motions co-exist. The results underscore the interplay between structural and fluidic nonlinearities in controlling the dynamic response of the fluttering disk in the post-flutter regime.
[DOI: 10.1115/1.1504097]

Introduction

The aeroelastic stability of rotating flexible disks is a significant concern for the engineering design of a diverse class of mechanical systems such as magnetic and optical data storage devices, thin sawblades, and turbomachinery. A majority of the literature on the problem is devoted to linear coupled fluid-structure interaction models aiming to predict accurately the speed and mode at the onset of aeroelastic flutter, [1–9].

To the best of our knowledge, [1,2,4,10] are the only works in the literature that present experimental data on the post-flutter vibration response of a spinning disk. In [1], the disk speed was changed in increments of 100 rpm, which is too large to resolve the transitions in dynamic response we are discussing here. It may

be noted that the disk and the experimental apparatus used here were also used in [1]. In [2] and [10] a focus was placed on investigating the onset of solitary waves on a very thin, membrane-like disk spinning over a thin air film. The results in [2] and [10] indicated a transition from harmonic to apparently fixed frequency solitary waves. This is similar to the frequency lock-in phenomenon described in the present work. However, in [2,10] the speed dependence of unstable wave amplitude, and the coexistence of multiple solutions in the post-flutter regime were not presented. The present experiments are performed using a stiff steel disk enclosed in a large sealed chamber, a significantly different experimental regime from [2] and [10].

This note aims to communicate rapidly experimental results, which describe the occurrence of new nonlinear dynamic phenomena occurring at rotation speeds above the onset of the flutter instability. These new results should assist the continuing development of nonlinear fluid-nonlinear structure interaction modeling for this problem.

Experimental Setup

The experimental apparatus (Fig. 1) utilized here is that used in [1]. The design minimizes sources of experimental error, including bearing noise, rotor imbalance, and unwanted stressing of the disk caused by temperature gradients. The primary elements include a thin disk held between thick collars, a high precision spindle, and vibration measurement instrumentation all placed inside a large, sealed chamber. The disk has a nominal outer diameter 356 mm, and the collar diameter is 106.7 mm. The disk material is 8660 steel, ground to a uniform thickness 0.775 mm and with maximum runout less than 0.10 mm. Residual stresses from manufacture are relieved after the grinding, creating a disk that is substantially stress-free. For further details of the experimental chamber and its functionality, the reader is referred to [1].

The experimental configuration in Fig. 2 shows two inductance-type displacement transducers measuring the transverse motion of the disk at a radial distance of 148 mm. The probes are angularly separated by 18 deg, have a linear range of 2.5 mm and a resolution of 0.20 μm . The vibration response signals from the two displacement probes are conveyed to a Tektronix 2630MS Modal Analyzer coupled to an IBM PS2/Model 70. A counter connected to an optical probe measures the disk rotation speed. An electromagnetic actuator is driven by amplified signals from the computer and applies a transverse force on the disk. Short duration pulses are applied to the actuator to investigate the stability of the fluttering motions under perturbation. The surrounding chamber is closed during the experiments.

Experimental Procedure

At pre-flutter speeds, disk vibration is excited randomly by the turbulent boundary layer that develops on the disk surface at high speeds. At each speed the Fourier spectrum of the vibration response is computed and averaged over ten time intervals. The magnitude of each peak is converted through the sensor calibration data to the amplitude of the corresponding traveling wave measured at the sensor location. Each peak in the vibration spectrum is associated with a (m, n) forward or backward traveling wave with m nodal circles and n nodal diameters. Identification of the nodal diameter number is facilitated through computation of the phase of the cross-spectrum of the data from the two displacement probes, [11].

As the disk speed is increased, the first critical speed occurs at 40.5 rev/s rotation speed. At this speed, the backward traveling wave (BTW) frequency of the (0,3) mode vanishes. With further increases in disk speed the (0,2), and (0,4) modes reach their critical speeds in succession. As the disk speed is increased into the supercritical range, the frequency of the (0,3) BTW increases from zero (This is sometimes called a reflected wave.) The amplitude of the peak corresponding to the (0,3) BTW starts to increase rapidly beyond 50 rev/s rotation speed indicating the onset of aeroelastic traveling wave flutter.

¹To whom correspondence should be addressed

Contributed by the Applied Mechanics Division of THE AMERICAN SOCIETY OF MECHANICAL ENGINEERS for publication in the ASME JOURNAL OF APPLIED MECHANICS. Manuscript received by the ASME Applied Mechanics Division, October 7, 2001; final revision, February 6, 2002. Associate Editor: N. C. Perkins.